# Inversion-Asymmetry and Warping-Induced Interband Magneto-Optical Transitions in InSb†

C. R. PIDGEON
*Francis Bitter National Magnet Laboratory,* Massachusetts Institute of Technology, Cambridge, Massachusetts 02139*

AND

S. H. GROVES‡
*Lincoln Laboratory, Massachusetts Institute of Technology, Lexington, Massachusetts 02173*

(Received 8 October 1968; revised manuscript received 5 March 1969)

Direct interband magneto-optical transitions have been observed at $\mathbf{k}=0$ in InSb using the reflection technique at 1.5°K. In addition to the normal spectral structure associated with allowed transitions, some strong features have been observed associated with "extra" transitions produced both by the warping and the linear-in-$\mathbf{k}$ splitting of the valence band of InSb. An unambiguous assignment of the origin of these transitions has been made by a study of the anisotropy of the spectra [with the magnetic field $\mathbf{H}$ in the (110) crystal plane] using left and right circularly polarized light. With the allowed and extra transitions, we can determine the relative energies of the first five valence-band magnetic energy levels. By fitting these, and the strengths of the extra transitions, we determine Luttinger's warping parameter $(\gamma_3-\gamma_2)$ and the Dresselhaus inversion-asymmetry parameter C. In addition, it is necessary to retain Luttinger's parameter $q$, which normally has been assumed to be zero. This quantity is present in the effective-mass Hamiltonian when there is a magnetic field and spin-orbit interaction. We find: $(\gamma_3-\gamma_2)=1.2\pm15\%$, $q=0.4\pm50\%$, and $C=6.6\times10^{-4}$ a.u. $\pm30\%$. This value of $C$ is about 4.5 times smaller than an erroneous value published previously.

## I. INTRODUCTION

In a previous treatment of interband magneto-absorption in InSb by Pidgeon and Brown[1] (referred to hereafter as I), the high-field measurements were interpreted in terms of a "quasi-Ge" model which included the nonparabolic and "quantum" effects in the conduction and valence bands, and most of the warping of the bands, but neglected the inversion asymmetry terms present in zinc-blende crystals (Dresselhaus,[2] Parmenter[3]). Weak fine structure observed in the spectra for the two directions of magnetic field under which the experiment was performed ($\mathbf{H}\|\langle100\rangle$ and $\langle110\rangle$) was accounted for by those warping terms which were initially omitted. These were included by perturbation theory following the approach of Luttinger[4] and Goodman.[5]

More recently, in a calculation of Landau levels in InSb, Bell and Rodgers[6] kept the full magnetic Hamiltonian for $\mathbf{H}\|\langle100\rangle$, including both second-order warping and inversion-asymmetry terms. The resulting infinite-order secular determinant was truncated to order 240×240 and then, with an assumed set of band parameters, solved with the aid of a computer for magnetic fields of 1 and 20 kOe. The results of this computation indicated that inversion-asymmetry–induced transitions should be observable in interband magneto-optical experiments in InSb.

The theory of the inversion-asymmetry terms—those of lowest order are the $k$ and $k^3$ terms—has been known for some time.[2,3,7] They result from the antisymmetric potential of the zinc-blende lattice and split the two-fold energy degeneracy at a given $\mathbf{k}$ value when there is a spin-orbit interaction. The splittings are small, and they have been difficult to observe experimentally. Recently it has been suggested that a beat frequency in the Shubnikov–de Haas effect in heavily doped $n$-type HgSe[8] gives the conduction-band inversion-asymmetry splitting,[9] and the same effect is apparently seen in $n$-type GaSb.[10] This has not been useful for determining the size of the term *linear in* $\mathbf{k}$, since at large $\mathbf{k}$ values both $k$ and $k^3$ terms contribute to the splitting of the $p$-like conduction band of HgSe, and $k^3$ terms to the splitting of the $s$-like conduction band of GaSb. Evidence of the linear-in-$\mathbf{k}$ splitting has been given by Robinson[11] from microwave cyclotron-resonance experiments in $p$-type InSb. However, difficulties in the interpretation of this type of experiment, resulting from poor resolution of the lines ($\omega_c\tau\sim0.9$) and the sensitivity to strain effects, make it desirable to have independent determinations. In addition, recent measurements of submillimeter cyclotron resonance by Button *et al.*,[12] in which seven lines were resolved,

† This work was sponsored by the U. S. Air Force.
* Supported by the U. S. Air Force Office of Scientific Research.
‡ Visiting scientist, Francis Bitter National Magnet Laboratory, Massachusetts Institute of Technology.

[1] C. R. Pidgeon and R. N. Brown, Phys. Rev. **146**, 575 (1966).
[2] G. Dresselhaus, Phys. Rev. **100**, 580 (1955).
[3] R. H. Parmenter, Phys. Rev. **100**, 573 (1955).
[4] J. M. Luttinger, Phys. Rev. **102**, 1030 (1956).
[5] R. R. Goodman, Phys. Rev. **122**, 397 (1961).
[6] R. L. Bell and K. T. Rogers, Phys. Rev. **152**, 746 (1966).
[7] E. O. Kane, J. Phys. Chem. Solids **1**, 249 (1957).
[8] C. R. Whitsett, Phys. Rev. **138**, 829 (1965).
[9] L. M. Roth, S. H. Groves, and P. W. Wyatt, Phys. Rev. Letters **19**, 576 (1967); L. M. Roth, Phys. Rev. **173**, 755 (1968).
[10] D. G. Seiler and W. M. Becker, Phys. Letters **26A**, 96 (1967).
[11] M. L. Robinson, Phys. Rev. Letters **17**, 963 (1966).
[12] K. J. Button, B. Lax, and C. C. Bradley, Phys. Rev. Letters **21**, 350 (1968).

demonstrated that the experiments of Ref. 11 and the earlier work of Bagguley *et al.*[13] measured only the envelope of the spectrum associated with the light and heavy hole. This is of relevance not only to the determination of the splitting linear in $\mathbf{k}$, but also to the measurement of valence-band anisotropy. Thus, an independent measurement of both these parameters is of interest.

In the present work we have used the interband magneto-optical method to investigate the interactions caused by the warping term and by the term linear in $\mathbf{k}$ of the $\mathbf{k}\cdot\mathbf{p}$ Hamiltonian for the valence band of InSb.[14] Direct valence to conduction-band magneto-optical transitions are studied in reflection at 1.5°K. Similar results using the electroreflectance technique will be reported elsewhere.[15] In addition to the normal structure associated with allowed transitions, some strong features are observed associated with warping-induced and inversion-asymmetry–induced transitions. As we show below, when the quantity $q$ (introduced by Luttinger) is nonzero, it also makes a contribution to the transitions which we call the warping-induced transitions. An unambiguous assignment of the origin of the extra transitions is made by a study of the anisotropy of the spectra, with $\mathbf{H}$ in the $(1\bar{1}0)$ crystal plane, using left and right circularly polarized light.

A matrix Hamiltonian linear in $\mathbf{k}$ has been given by Dresselhaus[2] in terms of $\mathbf{k}$ components along the crystallographic directions. We have extended this to the case of an external magnetic field in the $(1\bar{1}0)$ crystal plane showing that, as observed experimentally, the inversion-asymmetry–induced transition of interest is present for $\mathbf{H}\|\langle 111\rangle$ and $\langle 211\rangle$, but absent for $\mathbf{H}\|\langle 100\rangle$ and $\langle 110\rangle$. Weaker transitions by a factor of $\sim 5$ are also expected in the latter two directions, but these have not been observed experimentally. The same directional dependence is predicted and observed for the strong warping-induced transitions.

For our comparison of the observed transition energies with the theoretical Landau level energies it is necessary to consider the role of excitons. In the absence of a detailed quantitative theory for excitons associated with complex bands, we have had to make some reasonable assumptions about the energies. We discuss this problem briefly and make it clear what is being assumed.

To fit the relative energies of the first five valence-band magnetic energy levels we have to make small changes in the previously reported values of the higher-band interaction parameters $\gamma_1$, $\gamma_2$, $\gamma_3$, $\kappa$, and $q$. Of special interest, the quantity $q$, which has been put equal to zero in previous treatments, is needed for the fit of these first valence-band levels.

## II. THEORY

In I the magnetic energy levels for InSb were obtained by the method of Luttinger and Kohn[16] and Luttinger,[4] but with the modification that the conduction band was included with the valence bands in the coupled effective-mass equations. Here we are concerned with energy differences between transitions from levels at the top of the valence band to the *same* level in the conduction band (to the $n=0$ spin-up or spin-down conduction-band level). Since the valence-band levels of interest have very little conduction-band admixture, we work in the scheme of Ref. 4, which treats the valence band alone. Because of the large spin-orbit splitting, the split-off valence band is neglected as well. For the absolute energies of the transitions, we take the computed conduction-band levels from the coupled scheme of I, since the nonparabolic effect of the conduction band is then important.

The general form of the effective-mass Hamiltonian to order $k^2$ for the light- and heavy-hole valence bands in zinc-blende semiconductors is a $4\times 4$ matrix[17]

$$D=D^{+}+D^{-}, \tag{1}$$

where $D^{+}$ is the even part given by Luttinger,[4]

$$\begin{aligned}D^{+}=(\hbar^2/m)[&(\gamma_1+\tfrac{5}{2}\gamma_2)\tfrac{1}{2}k^2\\&-\gamma_2(k_x^2J_x^2+k_y^2J_y^2+k_z^2J_z^2)-2\gamma_3(\{k_x,k_y\}\{J_x,J_y\}\\&+\{k_y,k_z\}\{J_y,J_z\}+\{k_z,k_x\}\{J_z,J_x\})+(e/\hbar c)\kappa\mathbf{J}\cdot\mathbf{H}\\&+(e/\hbar c)q(J_x^3H_x+J_y^3H_y+J_z^3H_z)],\end{aligned} \tag{2}$$

and $D^{-}$ is the odd part (zero for materials with inversion symmetry),

$$\begin{aligned}D^{-}=-(2C/\sqrt{3})[&k_x\{J_x,V_x\}+k_y\{J_y,V_y\}\\&+k_z\{J_z,V_z\}].\end{aligned} \tag{3}$$

The notation is defined in Refs. 4 and 17. $\gamma_1$, $\gamma_2$, $\gamma_3$, $\kappa$, and $q$ are the effective-mass parameters for a Ge-type semiconductor; $C$ is the additional constant describing the interaction linear in $\mathbf{k}$; and $J_x$, $J_y$, and $J_z$ are $4\times 4$ angular momentum matrices for a state of spin $\frac{3}{2}$. When it is necessary to specify a representation for the $J$'s we use that of Ref. 4, Eq. (57). $\mathbf{k}$ is the kinetic momentum operator $[\mathbf{p}+(e/c)\mathbf{A}]$, where $\mathbf{A}$ is the vector potential of the external magnetic field. The symbol $\{a,b\}$ means the symmetrized product $\frac{1}{2}(ab+ba)$, and the quantities $V_x$, $V_y$, and $V_z$ are given by: $V_x=J_y^2-J_z^2$, $V_y=J_z^2-J_x^2$, and $V_z=J_x^2-J_y^2$. Some $k^3$ terms are also present in the valence band, but depend upon the presence of the admixed $s$-like conduction band. This admixing is not present for the levels involved in

[13] D. M. S. Bagguley, M. L. Robinson, and R. A. Stradling, Phys. Letters **6**, 143 (1963).

[14] C. R. Pidgeon and S. H. Groves, Phys. Rev. Letters **20**, 1003 (1968).

[15] C. R. Pidgeon and S. H. Groves, in *Proceedings of the Ninth International Conference on Physics of Semiconductors*, edited by S. M. Ryvkin (Nauka Publishing House, Leningrad, 1968), p. 307.

[16] J. M. Luttinger and W. Kohn, Phys. Rev. **97**, 869 (1955).

[17] G. Dresselhaus and M. S. Dresselhaus, in *The Optical Properties of Solids*, edited by J. Tauc (Academic Press Inc., New York, 1966), p. 198.

the transitions considered here, so we have not included these terms in $D^-$.

In general, the total wave function associated with Eq. (1) for the $n$th magnetic sub-band of a valence band $j$ is

$$\psi_j{}^n=\sum_{j'=1}^{4} u_{j'0}\sum_{n'=0}^{\infty}\alpha_{n'n}{}^{j'j}\Phi_{n'}, \tag{4}$$

where $u_{j0}$ is the band-edge cell-periodic part of the Bloch function for valence band $j$. $\Phi_{n'}$ is proportional to the one-dimensional harmonic-oscillator function of order $n'$. Because an infinite sum of harmonic-oscillator functions is needed to comprise the slowly varying envelope function which multiplies each $u_{j0}$, the dimension of the magnetic matrix Hamiltonian is infinite. To avoid this, one looks for cases in which Eq. (4) reduces to a single summation:

$$\psi_j{}^n=\sum_{j'}\alpha_n{}^{j'j}u_{j'0}\Phi_{n'}, \tag{5}$$

in which the $n'$ associated with $j'$ has a fixed relation to $n$ (e.g., $n'=n+1$). When Eq. (5) can be used the magnetic energy levels can be computed by diagonalizing a $4\times4$ matrix. A necessary condition for Eq. (5) is that the constant energy contours perpendicular to the direction of the magnetic field be circular. In general, this means that the anisotropic warping and inversion-asymmetry terms must be dropped from the magnetic Hamiltonian. However, Luttinger[4] has found ways of including the valence-band warping terms of order $k^2$. First, for the magnetic field along $\langle111\rangle$ directions the energy contours are circular in the $k_1k_2$ plane at $k_3=0$ (where $k_3$ is aligned along the magnetic field direction), and solutions in the form of Eq. (5) can be found. Second, Luttinger has found that most, but not all, the warping can be retained if the magnetic field is restricted to any direction of the $(1\bar{1}0)$ plane, which includes the high symmetry directions $\langle100\rangle$, $\langle110\rangle$, $\langle111\rangle$, and $\langle211\rangle$. Luttinger's approximate solution in this case is equivalent to having an isotropic mass in the $k_1k_2$ plane which is dependent upon the orientation of $k_3$ with respect to the crystallographic axes. Again the solutions are in the form of Eq. (5) but for every direction there is a perturbation Hamiltonian which contains the remaining anisotropy. Although this is usually small there are cases when the perturbation connects nearly degenerate Landau levels and a large amount of admixing of wave functions occurs.

In this paper it is convenient to use both the $(1\bar{1}0)$ plane solution and the $\langle111\rangle$ direction solution for $D^+$. The first shows the directional dependence of the extra warping transitions, but the second is more useful for estimating the strength of the warping, and the quantity $q$, from these transitions. The linear-in-$\mathbf{k}$ splitting, or $D^-$, is treated as a perturbation upon the eigenvalues of $D^+(\langle111\rangle)$. This treatment is justified in the high magnetic field region ($\mathbf{H}>20$ kOe), where these transitions are observed, since their strength is found experimentally to be at most one-tenth of that of the associated allowed transitions. One advantage of this is that it is possible to determine directly from experiment the size of the band parameter $C$.

We consider first the solution for $D^+$ for the $(1\bar{1}0)$ plane. For optical transitions we are interested in the energy at the top of each valence sub-band where there is a singularity in the joint density of states, so we set the component of momentum along the direction of the applied magnetic field, $k_3$, equal to zero. Following Ref. 4, $D^+$ is split into two parts for $\mathbf{H}$ in the $(1\bar{1}0)$ crystal plane,

$$D^+=D_0+(D_1+D_2). \tag{6}$$

The principal anisotropy is included in $D_0$ which has a solution in the form of Eq. (5). $D_1$, which contains the remaining warping, and $D_2$, which contains $q$, are treated as perturbations. $D_0$ decouples into two $2\times2$ blocks with envelope function solution:

$$f_{a,n}{}^{\pm}=\begin{pmatrix}a_{3,n}{}^{\pm} & \Phi_{n-2}\\ a_{5,n}{}^{\pm} & \Phi_n\end{pmatrix},\quad f_{b,n}{}^{\pm}=\begin{pmatrix}a_{6,n}{}^{\pm} & \Phi_{n-2}\\ a_{4,n}{}^{\pm} & \Phi_n\end{pmatrix}. \tag{7}$$

The notation of $I$ is used, where band-edge functions 1 and 2 are from the conduction band and do not appear here. These give rise to a light- and a heavy-hole ladder in the $a$ set and in the $b$ set. Here $+$ and $-$ refer to

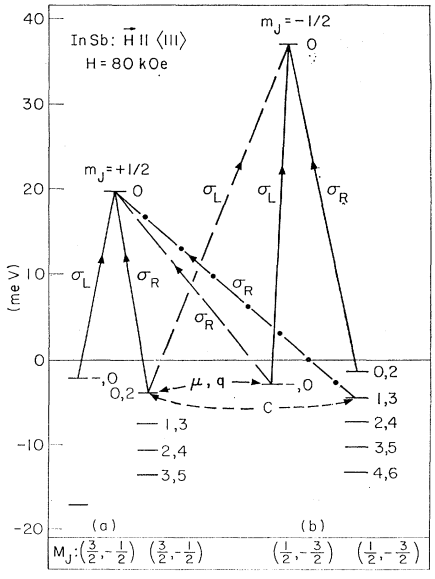


FIG. 1. Lowest magnetic energy levels for the valence and conduction bands of InSb. The numbers by the levels in the ($a$) and ($b$) valence ladders are the harmonic-oscillator numbers $n$ for the two-component wave functions (by convention, the largest number $n$ is used to label the level). The corresponding total angular momentum quantum numbers $M_J$ are given below. Allowed and extra transitions for the $\sigma_L(\Delta M_J=+1)$ and $\sigma_R(\Delta M_J=-1)$ spectra are shown: →— allowed, – –→– – warping induced, – · –→ inversion-asymmetry induced.

light- and heavy-hole solutions. The subscripts on the eigenvectors, $a$, refer to the associated band-edge cell-periodic functions, in a $(J,M_J)$ representation[16]:

$$\begin{aligned}
&(\tfrac{3}{2},\tfrac{3}{2}), \quad u_{3,0}(\mathbf{r})=|\,(1/\sqrt{2})(X+iY)\uparrow\rangle,\\
&(\tfrac{3}{2},-\tfrac{1}{2}), \quad u_{5,0}(\mathbf{r})=|\,-(1/\sqrt{6})[(X-iY)\uparrow+2Z\downarrow]\rangle,\\
&(\tfrac{3}{2},\tfrac{1}{2}), \quad u_{6,0}(\mathbf{r})=|\,(1/\sqrt{6})[(X+iY)\downarrow-2Z\uparrow]\rangle,\\
&(\tfrac{3}{2},-\tfrac{3}{2}), \quad u_{4,0}(\mathbf{r})=|\,-(1/\sqrt{2})(X-iY)\downarrow\rangle.
\end{aligned} \tag{8}$$

$a_{3,n}{}^{\pm}$ and $a_{6,n}{}^{\pm}$ equal zero for $n=0$ and 1. For higher $n$ values, each level is described by a two-component wave function, from Eq. (7), with associated quantum numbers $n$ and $(n-2)$. By convention we take the highest of these (i.e., $n$) as the quantum number label of the level. Allowed transitions, resulting from the diagonalization of $D_0$, then obey the selection rules $\Delta n=0$, $-2$. We define as extra transitions, those additional transitions which result from the inclusion of $D_1$, $D_2$, and $D^-$ in the Hamiltonian.

Energy levels calculated by the method of I, for the top of the valence band and bottom of the conduction band, are shown in Fig. 1. The solid lines show the allowed optical transitions that can take place for left and right circularly polarized light ($\sigma_L$ and $\sigma_R$) in the Faraday configuration ($\mathbf{E}\perp\mathbf{H}$): Electrons can be excited from the two $a$-set valence-band ladders into the $m_J=\frac{1}{2}$ conduction sub-band, or from the two $b$-set ladders into the $m_J=-\frac{1}{2}$ conduction sub-band.

### A. Warping-Induced Transitions

The explicit forms of $D_1$ and $D_2$ are given in Ref. 4, Eqs. (87) and (88). For $\mathbf{H}\|\langle 100\rangle$ and $\langle 110\rangle$, $D_1$ and $D_2$ decouple into two $2\times 2$ equations in the same way as $D_0$, thus mixing levels *within* either the $a$ or $b$ sets, but not *between* the two sets. It was shown in I that interband transitions produced by this mixing are in no case stronger than about one-tenth of the associated allowed transitions. However, for $\mathbf{H}\|\langle 111\rangle$ and $\langle 211\rangle$, $D_1$ and $D_2$ couple the $a$ and $b$ sets and can cause a large amount of admixing when the coupled $a$ and $b$ levels are close in energy. In this case, we must either include $D_1$ and $D_2$ with $D_0$ and diagonalize the Hamiltonian exactly, which can be done for $\mathbf{H}\|\langle 111\rangle$ [c.f. Eq. (62) of Ref. 4] or, alternatively, diagonalize the interaction between particular pairs of strongly interacting levels separately. For $\mathbf{H}\|\langle 111\rangle$ we have[4]

$$D_1(\langle 111\rangle)=\frac{-4}{\sqrt{6}}\left(\frac{ehH}{mc}\right)\mu\left\|\begin{matrix}0 & 0 & -\alpha^{\dagger 2} & 0\\ 0 & 0 & 0 & \alpha^{\dagger 2}\\ -\alpha^2 & 0 & 0 & 0\\ 0 & \alpha^2 & 0 & 0\end{matrix}\right\|\begin{matrix}\frac{3}{2}\\ -\frac{1}{2}\\ \frac{1}{2}\\ -\frac{3}{2}\end{matrix}, \tag{9}$$

and

$$D_2(\langle 111\rangle)=\left(\frac{ehH}{mc}\right)q\left\|\begin{matrix}23/8 & 0 & 0 & -1/\sqrt{2}\\ 0 & -13/8 & 0 & 0\\ 0 & 0 & 13/8 & 0\\ -1/\sqrt{2} & 0 & 0 & -23/8\end{matrix}\right\|\begin{matrix}\frac{3}{2}\\ -\frac{1}{2}\\ \frac{1}{2}\\ -\frac{3}{2}\end{matrix}, \tag{10}$$

with respect to the basis functions of Eq. (8). Here $\alpha^\dagger$ and $\alpha$ are the harmonic-oscillator creation and destruction operators, and $\mu=\frac{1}{2}(\gamma_3-\gamma_2)$. If for simplicity we first take $q=0$; we see that $D_1$ produces an interaction between two nearly degenerate levels in Fig. 1 giving rise to strong extra transitions to the $n=0$ conduction-band levels (shown by the dashed lines). The interacting levels are the lowest light-hole level in the $b$-set,

$$\psi_0=a_{4,0}{}^{+}\Phi_0 u_4, \tag{11}$$

and the lowest heavy-hole level in the $a$ set,

$$\psi_2=a_{3,2}{}^{-}\Phi_0 u_3+a_{5,2}{}^{-}\Phi_2 u_5 \tag{12}$$

(where the 0's on the $u$'s, indicating band-edge values, have been suppressed). With $q=0$, no other interactions with these levels are present (apart from the weak linear-in-$\mathbf{k}$ interaction considered in the next section) and we may treat this $2\times 2$ problem exactly. The interaction Hamiltonian is then

$$\mathcal{H}=\begin{pmatrix}\epsilon_0 & Q_{02}\\ Q_{20} & -\epsilon_0\end{pmatrix}, \tag{13}$$

where, from Eq. (9),

$$Q_{02}=-(4/\sqrt{3})\mu a_{4,0}{}^{+}a_{5,2}{}^{-}(ehH/mc), \tag{14}$$

and $2\epsilon_0$ is the energy separation between the unperturbed levels, with the zero of energy taken midway between them. The perturbed wave functions and energies are

$$\epsilon^{\pm}=\pm(\epsilon_0{}^2+Q_{02}{}^2)^{1/2}\equiv\pm\delta \tag{15}$$

and

$$\psi_2{}^{\pm}=e_0{}^{\pm}\psi_0+e_2{}^{\pm}\psi_2, \tag{16}$$

where $e_0{}^{\pm}$ and $e_2{}^{\pm}$ are given by

$$\begin{aligned}
e_0{}^{\pm}&=(\epsilon^{\pm}+\epsilon_0)/[Q_{20}{}^2+(\epsilon^{\pm}+\epsilon_0)^2]^{1/2},\\
e_2{}^{\pm}&=Q_{20}/[Q_{20}{}^2+(\epsilon^{\pm}+\epsilon_0)^2]^{1/2}.
\end{aligned} \tag{17}$$

Then the strength of the allowed transition (cf. Ref. I) is proportional to

$$[\langle\psi^-|\mathbf{p}\cdot\boldsymbol{\mathcal{E}}|\psi_c\rangle]^2=[e_2^-\langle\psi_2|\mathbf{p}\cdot\boldsymbol{\mathcal{E}}|\psi_c\rangle]^2, \quad (18)$$

and that of the extra transition to

$$[\langle\psi^+|\mathbf{p}\cdot\boldsymbol{\mathcal{E}}|\psi_c\rangle]^2=[e_2^+\langle\psi_2|\mathbf{p}\cdot\boldsymbol{\mathcal{E}}|\psi_c\rangle]^2, \quad (19)$$

where $\boldsymbol{\mathcal{E}}$ is a unit vector in the direction of the electric field of the incident radiation. We see that these both occur in the spectrum corresponding to $\sigma_R$ polarization of the incident radiation. $\psi_c$ is the wave function of the spin-up conduction-band level $\Phi_0S\uparrow$ (where $S$ is a function that transforms like an atomic $s$ function). The ratio of the strengths of extra to allowed transitions $x$ is

$$x=(e_2^+/e_2^-)^2, \quad (20)$$

hence from Eqs. (16) and (17) we obtain

$$Q_{02}^2=\delta^2\left[1-\left(\frac{1-x}{1+x}\right)^2\right]. \quad (21)$$

Thus, by determining experimentally the separation between, and ratio of the strengths of, extra and allowed transitions (i.e., $2\delta$ and $x$) we may obtain directly the warping parameter $\mu$ from Eq. (14).

It turns out, as will be shown in a later section, that $q$ is, in fact, nonzero. In this case, we have

$$Q_{02}=\left(\frac{ehH}{mc}\right)\left[\frac{-4}{\sqrt{3}}\mu a_{4,0}{}^+a_{5,2}{}^- -\frac{1}{\sqrt{2}}qa_{4,0}{}^+a_{3,2}{}^-\right]. \quad (22)$$

Thus, some of the simplicity is lost. The approach which will be taken below is to use all the available energy-level and transition-strength information to determine $\mu$, $q$ and the other parameters from a best-fit procedure. However, this simple two-level treatment shows the origin of the warping-induced transitions, and, further, is suitable for treating the interaction linear in $\mathbf{k}$ (Sec. II B).

By the argument used above we expect to see an extra warping-induced transition in the $\sigma_L$ spectrum from level (2) to the spin-down conduction-band level $\Phi_0S\downarrow$, shown by a second dashed arrow in Fig. 1.

The analysis given for $\mathbf{H}\|\langle111\rangle$ also applies to $\mathbf{H}\|\langle211\rangle$, since the form of $D_{1(\langle111\rangle)}$ is the same as that for $D_{1(\langle211\rangle)}$, with the addition of other coupling terms which can give rise to much weaker transitions.

With the source of these transitions recognized it is desirable to go to the eigenvalue problem for $\mathbf{H}\|\langle111\rangle$, where the warping and $q$ terms can be treated exactly. The solution to the effective-mass equation, $D^+{}_{(\langle111\rangle)}f=\epsilon f$, is

$$f_n{}^s=\begin{bmatrix}A_{3,n}{}^s\Phi_n\\A_{5,n}{}^s\Phi_{n+2}\\A_{6,n}{}^s\Phi_{n-2}\\A_{4,n}{}^s\Phi_n\end{bmatrix} \quad \text{for } n\geq 2,\ 3,\ \ldots, \quad (23)$$

where $s$ runs over the four ladders and the subscripts on the new eigenvectors, $A$, refer to the cell-periodic functions of Eq. (8).

### B. Inversion-Asymmetry-Induced Transitions

The explicit form of $D^-$ from Eq. (3) has been given by several authors for the case of $\mathbf{H}\|\langle001\rangle$ [i.e., the coordinate axes (1,2,3) aligned with the crystal axes]. For the case of $\mathbf{H}$ in any direction in the $(1\bar{1}0)$ crystal plane it is necessary to make the coordinate transformations given by Luttinger,[4]

$$\begin{aligned}
k_x&=(1/\sqrt{2})(ck_1-k_2),\\
k_y&=(1/\sqrt{2})(ck_1+k_2),\\
k_z&=-sk_1+ck_3,\\
J_x&=(1/\sqrt{2})(cJ_1-J_2+sJ_3),\\
J_y&=(1/\sqrt{2})(cJ_1+sJ_3),\\
J_z&=-sJ_1+cJ_3,
\end{aligned} \quad (24)$$

where $c=\cos\theta$, $s=\sin\theta$, and $\theta$ is the angle between $\mathbf{H}$ and the $z$ axis. The explicit forms of $D^-$ for the principal crystal directions with $k_3=0$ become

$$D^-(\langle100\rangle)=i\left(\frac{2eH}{3c\hbar}\right)^{1/2}C\left\|\begin{matrix}0&0&\frac{1}{2}\sqrt{3}\alpha^\dagger&\frac{3}{2}\alpha\\0&0&\frac{3}{2}\alpha&\frac{1}{2}\sqrt{3}\alpha^\dagger\\-\frac{1}{2}\sqrt{3}\alpha&-\frac{3}{2}\alpha^\dagger&0&0\\-\frac{3}{2}\alpha^\dagger&-\frac{1}{2}\sqrt{3}\alpha&0&0\end{matrix}\right\|\begin{matrix}\frac{3}{2}\\-\frac{1}{2}\\\frac{1}{2}\\-\frac{3}{2}\end{matrix}, \quad (25)$$

$$D^-(\langle110\rangle)=\frac{i}{4}\left(\frac{eH}{6c\hbar}\right)^{1/2}C\left\|\begin{matrix}-3(\alpha^\dagger-\alpha)&-\sqrt{3}(3\alpha^\dagger+5\alpha)&0&0\\\sqrt{3}(3\alpha+5\alpha^\dagger)&-9(\alpha^\dagger-\alpha)&0&0\\0&0&9(\alpha^\dagger-\alpha)&\sqrt{3}(3\alpha^\dagger+5\alpha)\\0&0&-\sqrt{3}(3\alpha+5\alpha^\dagger)&3(\alpha^\dagger-\alpha)\end{matrix}\right\|\begin{matrix}\frac{3}{2}\\-\frac{1}{2}\\\frac{1}{2}\\-\frac{3}{2}\end{matrix}, \quad (26)$$

and

$$D^-(\langle 111\rangle)=i\left(\frac{2eH}{3c\hbar}\right)^{1/2}C\begin{Vmatrix} 0 & -(1/\sqrt{2})\alpha^\dagger & \alpha & 0 \\ (1/\sqrt{2})\alpha & 0 & \sqrt{3}\alpha^\dagger & \alpha \\ -\alpha^\dagger & -\sqrt{3}\alpha & 0 & (1/\sqrt{2})\alpha^\dagger \\ 0 & -\alpha^\dagger & -(1/\sqrt{2})\alpha & 0 \end{Vmatrix}\begin{matrix} \frac{3}{2} \\ -\frac{1}{2} \\ \frac{1}{2} \\ -\frac{3}{2} \end{matrix}. \quad (27)$$

$D^-(\langle 211\rangle)$ has the same form as $D^-(\langle 111\rangle)$, but with some additional terms giving rise to additional weaker interactions between levels. These matrices agree with those of Ohmura.[18] In our original treatment we made an error in matrix representation with the result that Eq. (31) here differs from that in Ref. 14, and the size of the parameter $C$ previously reported is a factor of 4.5 too large.

We see by inspection that a strong interaction is possible for $\mathbf{H}\|\langle 111\rangle$ between nearly degenerate levels from the $a$ and $b$ sets [i.e., the lowest heavy-hole level (2) in the $a$ set and the second heavy-hole level (3) in the $b$ set]. This gives rise to the extra transition to the spin-up conduction-band level shown in Fig. 1 by the dot-dashed line, in the $\sigma_R$ spectrum. This interaction is also present for $\mathbf{H}\|\langle 211\rangle$, but is absent for the other two directions. Weaker interactions are also possible in the latter case, but these have not been observed experimentally. We use the same method as in the previous section to evaluate the interaction between the levels. As a result of the warping and $q$ interactions, level (2) has a three-component wave function, in terms of the eigenvectors of Eq. (23):

$$\psi_2=A_{3,0}^-\Phi_0u_3+A_{5,0}^-\Phi_2u_5+A_{4,0}^+\Phi_0u_4. \quad (28)$$

Level (3) is unaffected by the warping interaction and has the two-component wave function

$$\psi_3=A_{6,3}^-\Phi_1u_6+A_{4,3}^-\Phi_3u_4. \quad (29)$$

The interaction Hamiltonian is then

$$\mathcal{H}=\begin{Vmatrix} \epsilon_2 & Q_{23} \\ Q_{23}^* & -\epsilon_2 \end{Vmatrix}, \quad (30)$$

where

$$Q_{23}=i(2eH/3c\hbar)^{1/2}C[A_{3,0}^-A_{6,3}^-+\sqrt{(6)}A_{5,0}^-A_{6,3}^- +\sqrt{3}A_{5,0}^-A_{4,3}^--(\sqrt{\tfrac{1}{2}})A_{4,0}^+A_{6,3}^-], \quad (31)$$

and $2\epsilon_2$ is the energy separation between the unperturbed levels, with the zero of energy again taken midway between them. The appropriate form of Eq. (21) is then

$$|Q_{23}|^2=\bar{\delta}^2\left[1-\left(\frac{1-\bar{x}}{1+\bar{x}}\right)^2\right], \quad (32)$$

where $2\bar{\delta}$ is the experimentally measured separation between extra and allowed transitions, and $\bar{x}$ is the ratio of their strengths.

[18] Y. Ohmura, J. Phys. Soc. Japan **25**, 740 (1968).

## III. EXPERIMENTAL METHOD AND RESULTS

Conventional techniques were used for measuring magnetoreflection spectra of pure $n$-InSb ($N\sim10^{14}$ cm$^{-3}$), etched with a 5 to 10%, by volume, solution of bromine in methyl alcohol. The required spectral resolution was obtained with an InSb photovoltaic detector cooled to 77°K. In all cases the sample was submerged in superfluid helium at about 1.5°K. The experiments were carried out in the Faraday configuration ($\mathbf{E}\perp\mathbf{H}$) using a CsI Fresnel rhomb in conjunction with a AgCl pile of plates polarizer to achieve circular polarization. The window containing the superfluid helium was a sapphire disk oriented with the $c$ axis normal to its surface.

Reproducible results were obtained from a large number of samples of four different orientations: $\mathbf{H}\|\langle 100\rangle$, $\langle 110\rangle$, $\langle 111\rangle$, and $\langle 211\rangle$. Magnetoreflection spectra are shown in Fig. 2 for two directions of magnetic field. Because of the large conduction-band spin splitting, the transitions to the spin-up conduction sub-band (in the photon energy range 255–259 meV), and those to the spin-down sub-band (in the range 273–276 meV), are widely separated and permit unambiguous assignment. For $\mathbf{H}\|\langle 100\rangle$ and $\langle 110\rangle$ only the structure associated with the allowed transitions of Fig. 1 is observed, whereas in the other cases strong

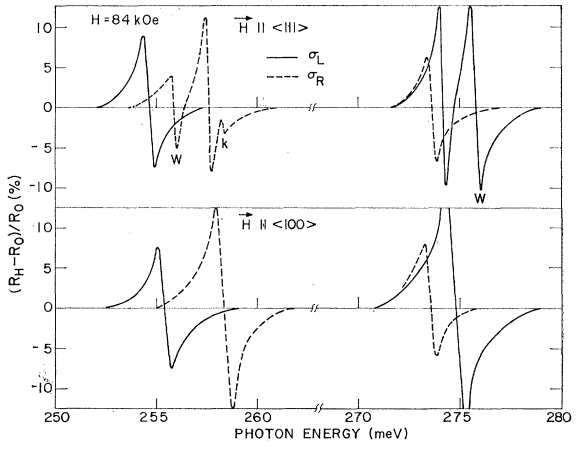


FIG. 2. Magnetoreflection spectra for $\mathbf{H}\|\langle 111\rangle$ and $\mathbf{H}\langle 100\rangle$ in the Faraday configuration, with $H=84$ kOe and $T=1.5$°K. Transitions to the $m_J=\frac{1}{2}$, $n=0$ conduction-band level occur to the left of the break in the energy scale and those to the $m_J=-\frac{1}{2}$, $n=0$, conduction-band level occur to the right. $w$ labels warping-induced transitions and $k$ labels the inversion-symmetry-induced transition.

additional structure associated with extra transitions appears. As predicted theoretically, the lowest allowed $\sigma_R$ transition separates into three components for $\mathbf{H}\|\langle 111\rangle$: warping-induced transition ($w$), allowed transition, and linear $\mathbf{k}$-induced transition ($k$). The second allowed $\sigma_L$ transition, near 275 meV, separates into an allowed and warping-induced ($w$) transition for $\mathbf{H}\|\langle 111\rangle$. Similar results are obtained for $\mathbf{H}\|\langle 211\rangle$. On some of the experimental traces (not that shown in Fig. 2) there is a very weak structure at about 277 meV, where it is expected that the mixing induced by the term linear in $\mathbf{k}$ should produce a transition, at reduced strength, to the spin-down conduction level.

A recorder trace, obtained by sweeping $\mathbf{H}$ at a fixed photon energy, is shown in Fig. 3 for $\mathbf{H}\|\langle 111\rangle$ and $\sigma_R$ polarization. Again the three component structure associated with warping-induced, allowed, and linear $\mathbf{k}$ transitions is clearly seen.

## IV. NUMERICAL RESULTS AND DISCUSSION

### A. Excitons

It is known on theoretical grounds (see Elliott and Loudon[19]) that the strong lines observed in interband magnetoabsorption experiments should be identified with transitions to exciton states associated with Landau levels. Experimental evidence for this has been given by Zwerdling *et al.*,[20] from magnetoabsorption measurements. The sharp dispersion-shaped reflectivity structure, shown in Figs. 2 and 3 (data of this type were first reported by Wright and Lax[21]), is seen for the lowest transitions in high-quality material. This line shape is suggestive of transitions to discrete levels

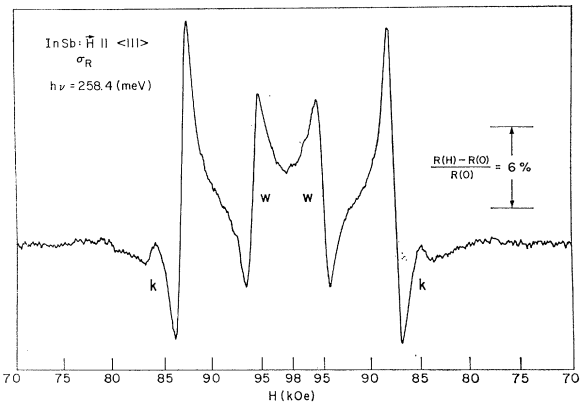


FIG. 3. Recorder trace for up- and down-field sweeps for the $\sigma_R$ transitions to the $m_J=\frac{1}{2}$, $n=0$ conduction-band level, at fixed photon energy. $w$ labels warping induced transitions and $k$ labels the inversion-asymmetry–induced transition.

(exciton) rather than of transitions between Landau sub-bands.

Recently Johnson[22] has identified the strong symmetric peak observed in magnetoabsorption with the creation of the exciton ground state, and a shoulder observed at slightly higher photon energy with the creation of the first excited state of the exciton. An estimate of the exciton binding energy can be made for a given value of $\mathbf{H}$ from the measured excited state energy, using a theory which is strictly applicable only to the case of simple energy bands. For the few transitions in which the excited state of the exciton is observable, this gives a means of comparing the exciton transition (the measured energy) with the Landau-level transition (the energy which can be theoretically computed from band parameters). Johnson studied the first two transitions in the Voigt configuration (i.e., to the $n=0$ spin-up and spin-down conduction band) for InSb. It was found that the separation between main peak and shoulder, $\delta\epsilon$, for these transitions increased smoothly with magnetic field in approximate agreement with the theoretical prediction of Ref. 19. An extrapolation of these results to the magnetic field used in the present work (84 kOe) yields the value for the transition to the spin-up level of $\delta\epsilon\uparrow\simeq 4.5$ meV, and for the transition to the spin-down level of $\delta\epsilon\downarrow\simeq 5.0$ meV.

In order to compare our measured and computed transition energies it is necessary to assume that the exciton binding energy for the transitions considered here, to the same conduction-band level, is the same (i.e., approximately equal to $\delta\epsilon\uparrow$ or $\delta\epsilon\downarrow$). This is reasonable since the effective masses (as determined both by the energy dependence on $\mathbf{H}$ and on $k_3$) of the levels in the valence band involved are about the same and about 20 times greater than the conduction-level mass. In addition, they all lie within an energy range of about 3 meV, whereas the conduction levels are separated by about 18 meV, owing to the large conduction-band $g$ factor.

Since we are concerned only with the *differences* in energy between transitions to the *same* conduction-band level—both for identifying the transitions, and for evaluating the interaction parameters of the previous sections—the over-all shift produced by the exciton binding energies should not then affect the interpretation in terms of Landau-level theory.

One possible source of difficulty with this arises if the exciton states interact. Consider the transitions, $T_1$ and $T_2$, from the two valence-band levels, $b^+(0)$ and $a^-(2)$—coupled through $\gamma_3-\gamma_2$ and $q$—to one of the $n=0$ conduction-band levels. With increasing energy we have two exciton ground states about 1.75 meV apart at 84 kOe, with their associated first excited states about 5 meV above the ground states. If $T_1$ is the lower energy transition, it is possible that

[19] R. J. Elliott and R. Loudon, J. Phys. Chem. Solids **15**, 196 (1960).
[20] S. Zwerdling, W. H. Kleiner, and W. P. Theriault, J. Appl. Phys. Suppl. **32**, 2118 (1961).
[21] G. B. Wright and B. Lax, J. Appl. Phys. Suppl. **32**, 2113 (1961).
[22] E. J. Johnson, Phys. Rev. Letters **19**, 352 (1967).

an excited state of $T_1$ may interact with the ground state of $T_2$ making the separation between exciton states less than the corresponding separation between valence-band Landau levels:

The following features of the spectra provide reassurance, but not proof, that this effect is not large. First, the measured energy separation between the ground states of transitions $T_1$ and $T_2$ is less than 2 meV at 84 kOe, while the energy of the $T_1$ first excited state is about 3 meV above the $T_2$ ground state. Second, we have found the relative strengths of the transitions to be independent of $H$, and the relative energies to vary linearly with $H$ in the range 30 to 100 kOe. Thirdly, because $\delta\epsilon\uparrow$ and $\delta\epsilon\downarrow$ are not equal, a strong exciton interaction might be expected to give different values for the difference of the transition energies $T_1-T_2$ to the spin-up and spin-down $n=0$ conduction levels. A more sensitive indicator is the ratio of warping-induced to allowed transition strengths $x$, which we see from Fig. 2 is about 0.5 for the spin-up conduction band and 1.0 for the spin-down band. Equation (21) shows that these should be the same for a simple two-level interaction; but also, that in this range of $x$, a small change in $\delta$ makes a very large change in $x$ for a fixed interaction strength (i.e., a 6% change in $\delta$ would account for the different experimental values of $x$). Thus, the difference in the very sensitive indicator, $x$, may be due to the exciton interaction which we have assumed to be nonexistant. By the same argument, however, the determination of $Q_{02}$—and hence the band parameters—is insensitive to the difference in $x$ found here. This, again, is reassuring, but is not proof that the total effect is negligible.

### B. Band Parameters

In Fig. 2 we find the linear $\mathbf{k}$ and warping-induced transitions for $\mathbf{H}\|\langle 111\rangle$, predicted from Fig. 1. It is worth summarizing the steps leading to the assignment:

(1) The basic energy band level scheme, and identification of the allowed transitions, is known from I.

(2) From the relative energies of the allowed and extra transitions in the $\langle 111\rangle$ case, we identify the valence-band levels of origin.

(3) Equation (1) shows that the only interactions present between the pairs of levels involved (Fig. 1), which will also give rise to transitions to the $n=0$ conduction-band levels in the polarizations found experimentally, are the inversion-asymmetry and warping interactions.

We use a slightly different procedure from that used in Ref. 14 to make a quantitative fit of the spectra. There we essentially used Eq. (21) to get the observed separation between interacting states and intensity ratio of extra and allowed transitions. Actually, the strength of the warping was determined using the exact solution of $D^+\langle 111\rangle$, but the requirement for the fit was in terms of the separation of just the two interacting levels. More recently we have been concerned with fitting the relative energies of all the first five valence levels in Fig. 1 from which transitions can be made to the $n=0$ conduction levels. We find that, when the parameter $q$ in Eq. (22) is taken to be zero, it is possible to bring only four of these valence levels into a reasonable fit with experiment; a significant discrepancy remains for the first heavy-hole level in the $b$ set. From experiment we expect this to be about 0.5 meV above the first light-hole level in the $b$ set, whereas the theory predicts about 1.5 meV. When $q$ is allowed to vary, all of the five levels can be brought into agreement with experiment with a best-fit procedure.

The higher-band parameters reduce to individual higher-band interactions as follows[23]:

$$\begin{aligned}\gamma_1&=-\tfrac{1}{3}(F'+2G+2H_1+2H_2)-1,\\ \gamma_2&=-\tfrac{1}{6}(F'+2G-H_1-H_2),\\ \gamma_3&=-\tfrac{1}{6}(F'-G+H_1-H_2),\\ \kappa&=-\tfrac{1}{6}(F'-G-H_1+H_2)-\tfrac{1}{3},\end{aligned}\tag{33}$$

where, in the representations of the diamond lattice,

$$\begin{aligned}F'&=(2/m)\sum_j^{\Gamma_{2'}}|\langle X|p_x|u_{j,0}\rangle|^2/(\epsilon_v-\epsilon_j),\\ G&=(1/m)\sum_j^{\Gamma_{12'}}|\langle X|p_x|u_{j,0}\rangle|^2/(\epsilon_v-\epsilon_j),\\ H_1&=(2/m)\sum_j^{\Gamma_{15}}|\langle X|p_y|u_{j,0}\rangle|^2/(\epsilon_v-\epsilon_j),\\ H_2&=(2/m)\sum_j^{\Gamma_{25}}|\langle X|p_y|u_{j,0}\rangle|^2/(\epsilon_v-\epsilon_j),\end{aligned}\tag{34}$$

and $\epsilon_v$ is the valence-band-edge energy. A discussion of the $\mathbf{k}\cdot\mathbf{p}$ makeup of $q$ is given in the Appendix. The prime on $F$ indicates that the conduction band is to be excluded from the sum, since it is not a higher band in our treatment. Thus, $F$ is a large quantity and $F'$ very much smaller.

The heavy-mass band has no interaction with bands of symmetry $\Gamma_{2'}$, so that we expect the heavy-hole levels in Fig. 1 to be insensitive to $F$. As has been mentioned previously, the first light-hole levels have heavy-hole character, meaning that these also are insensitive to $F$. Thus, the best-fit procedure to the relative spacing of the first five valence levels determines the band parameters of Eq. (33) only to within some constant which adds to them as $F'$. For example, if a constant $X$ is added to $\gamma_1$, then $\frac{1}{2}X$ must be added to $\gamma_2$, $\gamma_3$, and $\kappa$. We note that the warping parameter $\gamma_3-\gamma_2$ is independent of this. $q$ also is independent of such a shift.

[23] L. M. Roth, B. Lax, and S. Zwerdling, Phys. Rev. **114**, 90 (1959).

To fix the absolute values of the higher-band parameters, i.e., to determine the quantity $X$, we go to the earlier magnetoabsorption data of I and adjust $X$ for a best fit, using the coupled 8×8 Hamiltonian matrix. We obtain the following results:

$$\gamma_1=3.60,\quad \gamma_2=-0.47,\quad \gamma_3=0.70,$$
$$\kappa=-1.48,\quad q=0.39.$$

This leads from Eq. (33) to the values: $F'=0$, $G=-1.31$, $H_1=-5.59$, and $H_2=0$. The best-fit procedure gives values of the $\gamma$'s, $\kappa$, and $q$ directly, which, from Eq. (33), lead to a small positive value of $H_2$. Since the $\Gamma_{25}$ levels derive from $f$-like atomic orbitals and the lowest $f$-like orbitals ($4f$) are thought to lie at much higher energies than the $5p$ valence orbitals, $H_2$ should be small and negative. The values above are from a best fit with the restraint $H_2\leq 0$. This causes some deterioration in the fit, giving at worst a difference of 0.15 meV between observed and predicted energies at 84 kOe. When the $H_2\leq 0$ restraint is removed we find: $\gamma_1=3.83$, $\gamma_2=-0.45$, $\gamma_3=0.87$, $\kappa=-1.7$, and $q=0.57$, giving some idea of the change which noticeably worsens the fit. The lower limit of the error on the quantity $X$ was obtained from the theoretical requirement $F'\leq 0$; we estimate the upper error limit to be about 6%. We have used the value $\epsilon_G=0.2366$ eV given by Johnson,[22] and determined the value $P^2=0.390$ a.u. from the over-all best fit of the magnetoabsorption data. The resulting Luttinger band parameters[4,1] are: $\gamma_1^L=33.51$, $\gamma_2^L=14.48$, $\gamma_3^L=15.65$, $\kappa^L=13.47$, and $q^L=q=0.39$. The first four of these are slightly different from those given in I, where it was necessary to assume a value for the heavy mass from cyclotron-resonance measurements[13]; the fifth parameter $q$ is determined here for the first time. The classical

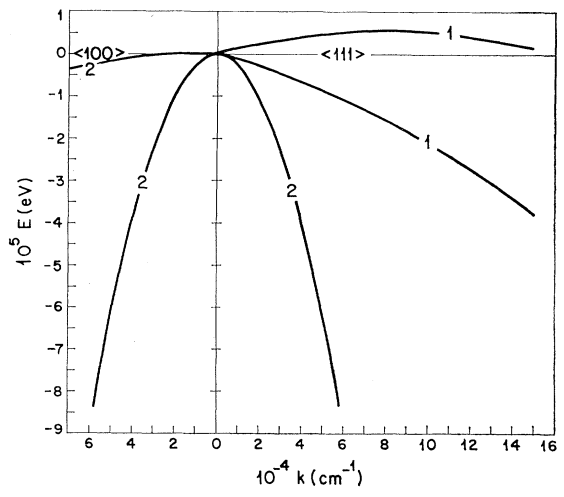


FIG. 4. Valence-band dispersion relations for **k** along ⟨100⟩ and ⟨111⟩ directions using the value of the parameter $C$ determined here. The numbers indicate the degeneracy of the band. In all other directions both light- and heavy-mass bands are split. The maximum splitting occurs for the ⟨111⟩ heavy-mass band.

(large Landau-level number) cyclotron masses for the heavy-hole band which come from using the best-fit parameters above and the theoretical expressions from $D_0$ [Eq. (6)] are: $m(\langle 100\rangle)=0.273m$, $m(\langle 110\rangle)=0.332m$, and $m(\langle 111\rangle)=0.358m$ with an error of $\sim\pm 0.005m$.

Finally, from the relative strength and energy separation of the allowed and inversion-asymmetry–induced transitions, $C$ may be determined directly from Eqs. (22), (31), and (32), using the exact solution to $D^+(\langle 111\rangle)$ obtained above. The uncertainty in the size of $C$ comes from the uncertainty in $x$, the strength ratio. With $x=0.05$ we find $C=6.6\times 10^{-4}$ a.u. or $9.3\times 10^{-11}$ eV cm. An error of ±30% includes the range $x=0.1$–$0.025$. As mentioned earlier this is about 4.5 times smaller than an erroneous value published previously.[14] Our result for $C$ is about an order of magnitude smaller than that given in Refs. 6 and 11, and a factor of 5 smaller than the theoretical estimate of Kane.[7]

The revised valence-band $\epsilon(\mathbf{k})$ dispersion relations for **k** along ⟨100⟩ and ⟨111⟩ directions are shown in Fig. 4. The maximum upbending of the heavy-hole band is about $5\times 10^{-6}$ eV. For the warping parameter we find $(\gamma_3-\gamma_2)=1.2\pm 15\%$. Owing to the inclusion of $q$ in the fitting procedure, the result for $(\gamma_3-\gamma_2)$ is slightly different from that given in Ref. 14. It remains in good agreement with the cyclotron-resonance work of Bagguley *et al.*,[13] and not with the more recent work of Tohver and Ascarelli[24]; although, as pointed out by Button *et al.*,[12] the heavy-hole transition observed by these workers represents only the envelope of several different lines, so the comparison with our results is probably not meaningful.

At low magnetic fields the terms linear in **k** will have a large perturbing effect on the magnetic energy levels, and the perturbation approach discussed here will break down. In this case an energy-level calculation such as that described in Ref. 6 becomes necessary, and it may even be necessary to use the off-($\mathbf{k}=0$) approach of Ohmura.[18] However, the small size of the inversion-asymmetry transition observed experimentally justifies our approach. We have seen this transition in the region from 30 to 100 kOe, where the small perturbation method is found to be valid.

In conclusion, we have found experimentally that the inversion-asymmetry terms in the valence band do not represent a large perturbation on the quasi-Ge scheme of I in the high-field limit (i.e., for fields greater than about 20 kOe), so that the latter approach is a valid method for calculating the Landau levels in InSb. However, the second-order warping interaction may become extremely strong for directions of magnetic field other than $\mathbf{H}\|\langle 100\rangle$ and ⟨110⟩, and must be treated explicitly, as discussed in this paper.

[24] H. T. Tohver and G. Ascarelli, in *Proceedings of the Ninth International Conference on Physics of Semiconductors*, edited by S. M. Ryvkin (Nauka Publishing House, Leningrad, 1968), p. 326.

## ACKNOWLEDGMENTS

We are grateful for helpful discussions to K. J. Button, J. O. Dimmock, G. Dresselhaus, E. J. Johnson, B. Lax, J. Mavroides, and L. M. Roth. We wish to thank J. Casteris and J. McNally for experimental assistance.

## APPENDIX A: ESTIMATE OF $q$ FOR InSb

As shown by Hensel and Suzuki,[25] $q$ arises from the spin-orbit splitting of the $\Gamma_{15}$ conduction band $\Delta_{15}$, and will be comparable to the other higher-band parameters when this splitting is a non-negligible fraction of the $\Gamma_{15}-\Gamma_8^+$ energy separation, $\epsilon_{15}-\epsilon_v$. Their expression for $q$ is the following:

$$q=(4/9m)|\langle X|p_y|u_{15,0}\rangle|^2\Delta_{15}/(\epsilon_{15}-\epsilon_v)^2.$$

Then, from Eq. (34),

$$q\simeq-(2/9)H_1\Delta_{15}/(\epsilon_{15}-\epsilon_v),$$

where we have made the approximation that only the lowest $\Gamma_{15}$ band contributes to $H_1$. If we assume that $\Delta_{15}\simeq\Delta=0.8$, and take the estimate of Herman *et al.*[26] for $\epsilon_{15}-\epsilon_v\simeq3.8$ eV, this leads to $q\simeq0.3$. Considering the uncertainties in these quantities this is adequate agreement with the value we find experimentally.

[25] J. C. Hensel and K. Suzuki, Phys. Rev. Letters **22**, 838 (1969).

[26] F. Herman, R. L. Kortum, C. D. Kuglin, J. P. Van Dyke, and S. Skillman, in *Methods of Computational Physics*, edited by B. Alder, S. Fernback, and M. Rotenberg (Academic Press Inc., New York, 1968).

## APPENDIX B: INTERBAND AND INTRABAND DETERMINATION OF MASS PARAMETERS

The heavy-hole effective mass determined here is about 10% lighter than the corresponding cyclotron-resonance determinations.[12,13,24,27] Further, the conduction-band mass is about 5% heavier than that determined in cyclotron resonance (c.f. Dickie *et al.*[28] and Summers *et al.*[29]). These discrepancies between masses determined from interband and intraband experiments may be characteristic of a more general situation. For example, recent interband measurements on grey tin[30] show similar discrepancies with earlier intraband measurements[31] for the conduction- and valence-band masses. In addition the conduction-band $g$ value of InSb as determined by electron spin resonance (Bemski,[32] Isaacson[33]) does not agree with that determined by interband magnetoabsorption (Pidgeon *et al.*[34]); further, both determinations are inconsistent with the cyclotron-resonance effective mass[28,29] if one uses the simple formula given by Roth *et al.*[23] for the band-edge $g$ value.

These problems have not yet been explained and deserve to receive additional experimental and theoretical study.

[27] K. J. Button, A. Brecher, B. Lax, and C. C. Bradley (to be published).

[28] D. H. Dickie, E. J. Johnson, and D. M. Larson, Phys. Rev. Letters **18**, 599 (1967).

[29] C. J. Summers, R. B. Dennis, B. S. Wherrett, P. G. Harper, and S. D. Smith, Phys. Rev. **170**, 755 (1968).

[30] S. H. Groves, C. R. Pidgeon, A. W. Ewald, and R. J. Wagner (to be published).

[31] B. L. Booth and A. W. Ewald, Phys. Rev. **168**, 796 (1968).

[32] G. Bemski, Phys. Rev. Letters **4**, 62 (1960).

[33] R. A. Isaacson, Phys. Rev. **169**, 312 (1968).

[34] C. R. Pidgeon, D. L. Mitchell, and R. N. Brown, Phys. Rev. **154**, 737 (1967).